

Two Bathointermediates of the Bacteriorhodopsin Photocycle, Distinguished by Nanosecond Time-Resolved FTIR Spectroscopy at Room Temperature

Andrei K. Dioumaev and Mark S. Braiman*

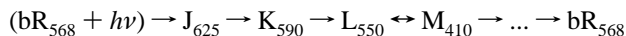
Department of Biochemistry, University of Virginia Health Sciences Center, Charlottesville, Virginia 22908

Received: May 23, 1996; In Final Form: December 13, 1996[®]

FTIR step-scan spectroscopy with 10 ns nominal time resolution was applied to the early stages of the photocycle of bacteriorhodopsin at room temperature. Kinetic data analysis with global fitting revealed two distinct bathointermediates prior to relaxation into the L state. The late bathointermediate (which we term K_L) is the K state as originally defined by Lozier *et al.* (*Biophys. J.* **1975**, *15*, 955). The earlier bathointermediate, K_E , decays to K_L with an apparent time constant of 640 ± 90 ns at 5 °C; this decay process is approximately 50–100 ns at 25 °C. The transient change in vibrational difference bands associated with this transition are spread throughout the 1800–800 cm^{-1} range. However, the largest differences in the spectra of K_E and K_L appear to be mostly associated with a relaxation of the Schiff base end of the retinal chromophore and/or its immediate environment. Both our K_E and K_L IR spectra are different from the spectra of bathoproducts obtained at cryogenic temperatures. Our fitted time constants also imply that neither of these intermediates (K_E and K_L) can be identified with the K or KL states as defined by Shichida *et al.* (*Biochim. Biophys. Acta* **1983**, 723, 240), and consequently, our spectra for K_E and K_L are markedly different from IR spectra calculated for those states by Weidlich and Siebert (*Appl. Spectrosc.* **1993**, 47, 1394) and Sasaki *et al.* (*Biophys. J.* **1995**, 68, 2073). That is, here we characterize a new nanosecond bathointermediate, K_E , in the bacteriorhodopsin photocycle under physiological conditions, which was not detected in previous studies.

Introduction

Bacteriorhodopsin, a natural retinal protein from *Halobacterium salinarum*, acts as light-induced proton pump. (For a review see refs 1 and 2.) The early stages of the photocycle are usually described as a sequence of the following intermediates:^{3–6}



Here the subscripts indicate approximate wavelength in nanometers of the maximal absorption in the visible. The K state is formed at room temperature with a time constant of approximately 3–5 ps^{7,8} and is commonly referred to as a bathointermediate due to the bathochromic (red) shift of its main visible absorption band. The L state is formed with a time constant of $\sim 1 \mu\text{s}$.^{4,9–13}

K-like states have been characterized both by static spectroscopy at low temperature^{3,14–22} and by time-resolved spectroscopy at room temperature with either picosecond^{7,8,23–27} or submicrosecond time resolution.^{3,9,11,22,28,29} In spite of the fact that these different experimental methods result in different spectral characteristics for the bathointermediate produced under various conditions, one and the same name—K—has been historically used for all those states.

Differences between these K states have been noted, based on UV and visible,^{30–33} FTIR,^{19,34} resonance Raman (RR),^{24,25,35} and photoelectric³⁶ measurements in the temperature range from –196 to +20 °C. While there is a general consensus that these differences are real and reproducible, there are conflicting reports on their interrelationship and on the dynamics of the bacteriorhodopsin photocycle in the 10 ps to 500 ns time range. To explain some of these differences, a new transition between K states was proposed, and the two substates were termed K and K_L .³⁷

The differences between various K states are more distinct in vibrational (RR and FTIR)^{24–27,34,35,38} than in visible absorption^{12,13,37,39} spectra. However, until recently, vibrational spectroscopists have had to rely on previously published kinetic properties (obtained mostly by spectroscopy in the visible) for assignment and separation of intermediates. Therefore, introduction of the distinct K and K_L states³⁷ led to attempts to characterize these states by IR and RR.^{19,26} The resulting characterizations are questionable, because the kinetic assumptions that went into them were later shown to be erroneous.^{13,39} That is, calculations based on the nonexistent ~ 10 ns transition between K and K_L states, and subsequent comparison with low-temperature spectra of the K state, has led to confusion in assignments of IR peaks to early and late K states.^{22,29,40,41}

In a series of articles based on ~ 100 ns time-resolved IR measurements,^{29,40,41} two bathointermediates were characterized at room temperature. These were again called K and K_L , assuming the sequence $\text{K} \rightarrow \text{KL} \rightarrow \text{L} \rightarrow \dots$ of Shichida *et al.*³⁷ The only detected IR spectral difference between these two states was in their HOOP peaks: 958 cm^{-1} for K and 984 cm^{-1} for K_L .⁴¹ There are three main reasons to question the published interpretations of these IR kinetic results:

1. The measurements were performed with 20 ms spacing between the excitation flashes. This inevitably leads to accumulation of long-lived intermediates. The longest apparent time constant for similarly prepared samples is 26.4 ms.⁴² Long-lived photointermediates are photolabile,⁴³ creating additional intermediates with relaxations in the nanosecond time domain.⁴⁴ No attempt was made to separate these secondary effects in the nanosecond time-resolved reports,^{29,40,41} making it unclear whether the reported spectral and kinetic features belong to the intermediates of the native photocycle or are due to additional intermediates created by double excitation.

2. The high level of noise in the published time-resolved IR spectra suggests that spectral changes at wavenumbers > 1000

[®] Abstract published in *Advance ACS Abstracts*, February 15, 1997.

cm^{-1} might be detected in the nanosecond time range if only the signal-to-noise ratio were improved.

3. The time constant for the $K \rightarrow KL$ transition was claimed to be ~ 10 ns,⁴¹ obtained by deconvolution from transient signals measured with a 60 ns (fwhm) instrumental rise time. The chances for correct estimation of the time constant for a chemical reaction (τ_{reaction}) decrease when it becomes shorter than the instrumental rise time ($\tau_{\text{instrument}}$) of the measuring apparatus. In this particular case,⁴¹ $\tau_{\text{instrument}}/\tau_{\text{reaction}}$ was ~ 6 , requiring a signal-to-noise ratio at least $e^6 \cong 400$ for deconvolution. However, the reported signal-to-noise ratio was far lower than this. This raises the question of whether the reported ~ 10 ns time constant⁴¹ is an artifact or really present in the data.

These shortcomings have led us to reinvestigate the kinetics and IR spectra of the early stages of the bacteriorhodopsin photocycle. Here we present a time-resolved FTIR study on the photocycle from 10 ns to 50 μs for a broad (1800–800 cm^{-1}) spectral range, with a signal-to-noise ratio adequate to distinguish definitively the spectral differences between two K states, as well as to measure the time constant for the transition between them. The latter is at least 5 times slower than the previously reported experimental estimates.

Materials and Methods

Bacteriorhodopsin (bR) used was in the form of purple membranes from the S9 strain of *Halobacterium salinarum*. The bR was harvested and purified according to a published procedure,⁴⁵ without using the sucrose density gradient. The samples for IR measurements were prepared in 25 mM Tris-HCl buffer (pH 7.3, in the presence of 100 mM NaCl) and squeezed between BaF₂ windows (25 mm diameter, 2 mm thickness) as described previously.⁴⁶ The water content of the samples (~ 50 – 80% w/w) was estimated from the ratio of absorbance at ~ 1650 and ~ 1555 cm^{-1} .⁴⁶

Time-resolved FTIR spectra with 10, 50, and 100 ns spacing between time slices were measured on a Bruker IFS-66 (Bruker Analytische Messtechnik GmbH, Karlsruhe, Germany) step-scan spectrometer. Data collection at 8 cm^{-1} resolution for an 800–1800 cm^{-1} spectral range was controlled by the OPUS/IR (V 2.2) software of the IFS-66 spectrometer. The temperature was controlled with a refrigerated water bath (RT-110, Neslab, Portsmouth, NH) and a temperature-controlled IR cell (Harrick, Ossining, NY).

All measurements were done with an HgMnTe photovoltaic detector and amplifier with ~ 40 ns rise time (KMPV11-1-LJ2/239; Kolmar Technologies, Conyers, GA). The ac-coupled output of the preamplifier was amplified by an external amplifier with 300 MHz bandwidth (SR445, Stanford Research Systems, Sunnyvale, CA) and digitized by the first channel of the external transient recorder of the IFS-66 spectrometer. The corresponding dc-coupled output of the preamplifier was simultaneously fed into the second channel of the transient recorder and was saved for subsequent phase correction during the Fourier transformation of the ac-coupled signal.

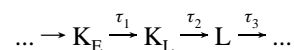
Photoexcitation was by the 532 nm second harmonic of a pulsed Nd:YAG laser (Quanta-Ray GCR-11, Spectra-Physics, Mountain View, CA). The repetition rate of the excitation was 1 Hz at 5 °C and 5 Hz at 25 °C. That is, the spacing between flashes was several times greater than the slowest time constants detected on similar sample preparations.⁴² This prevented accumulation of late intermediates in the photocycle. To minimize light-induced sample degradation,^{47,48} the excitation flash intensity was ~ 4 – 12 mJ/cm^2 , and the sample was replaced after each 140 000 flashes (at 25 °C) or 30 000 flashes (at 5 °C).

Final results were obtained by averaging $\sim 6 \times 10^5$ flashes at 25 °C and $\sim 1.2 \times 10^5$ flashes at 5 °C, using data from four separate experiments at each temperature. This resulted in a noise level of ~ 350 μOD in individual 10 ns time slices (at 25 °C) and ~ 200 μOD for the 50 ns time slices (at 5 °C).

Kinetic data analysis was performed by nonlinear least-squares global fitting to multiexponentials using the program FITEXP.⁴⁹ Prior to fitting, the data were condensed by averaging to a quasi-logarithmic time base with ~ 13 time points per decade. After fitting, the noise level in the calculated spectra was ~ 40 and ~ 80 μOD for 50 and 10 ns time-resolved data, respectively.

These fits yield the best approximation of measured data, $\Delta I(\nu_j, t)$, in the form $\Delta I(\nu_j, t) = \sum \{B_i(\nu_j, i) \exp[-t/\tau_i]\} + B_0$, where τ_i are the time constants of kinetic process and $B_i(\nu_j, i)$ are the corresponding amplitudes of these processes. (That is, the time constant τ_i was constrained to be the same at all ν_j for the i th process.) The number of detected transient states was determined by applying F -test statistics.^{49,50}

Each particular fitted amplitude spectrum, $B_i(\nu_j, i)$, corresponds to an apparent decay process, rather than to any pure difference spectrum of a particular intermediate. The difference spectra of intermediates presented below were calculated from the amplitude spectra assuming the simplest sequential unidirectional photocycle scheme:



All time-resolved data were measured and fitted as “single beam spectra”, $\Delta I(\nu, t)$. Only for the calculated intermediates’ spectra below were these data converted to absorption changes $\Delta A(\nu, t) = -\log\{1 + \Delta I(\nu, t)/I_0(\nu)\}$, where $I_0(\nu)$ was the static single beam spectrum of the same sample measured prior to time-resolved measurements in the rapid scan mode (averaging 10^3 scans). Each spectrum is presented as an absorbance difference between a particular intermediate or mixture of intermediates (positive peaks) and the unphotolyzed bR state (negative peaks), but will often be referred to just by the name of the photointermediate(s).

Results

Figure 1 presents IR difference spectra measured with 10 ns per time slice at 25 °C. An analogous set of data, measured with 50 ns per time slice at 5 °C, is presented in Figure 2. Kinetic analysis (see below) of data sets at 5 and 25 °C allowed us to obtain IR difference spectra of four intermediates. On the basis of their kinetic and spectral characteristics, we associate these intermediates with two distinct K-like states, as well an L-like and an M-like state.

Kinetic Analysis. Global multiexponential fitting of data covering the range 800–1800 cm^{-1} and 0.3–40 μs at 5 °C revealed two processes, with time constants $\tau_1 = 640 \pm 90$ ns and $\tau_2 = 7 \pm 2$ μs . These processes were preceded by an instrumentally limited rise time, τ_0 . The instrumental rise is nonexponential; its fwhm is ~ 40 ns. Increasing the temperature to 25 °C results in an acceleration of τ_2 to 0.8 ± 0.2 μs , and the appearance of one additional process in the 0.3–50 μs range, with a time constant of $\tau_3 = 16 \pm 4$ μs . However, τ_1 is reduced to ~ 50 – 100 ns, and its accurate deconvolution from the instrumental rise (with $\tau_0 \approx 40$ ns) becomes problematic.

On the basis of their absolute values and temperature dependence, we correlate the slowest two of our three observed time constants to known relaxation processes of the bacteriorhodopsin photocycle. The τ_3 process (16 ± 4 μs at 25 °C) is in accord with a kinetic process described earlier by time-

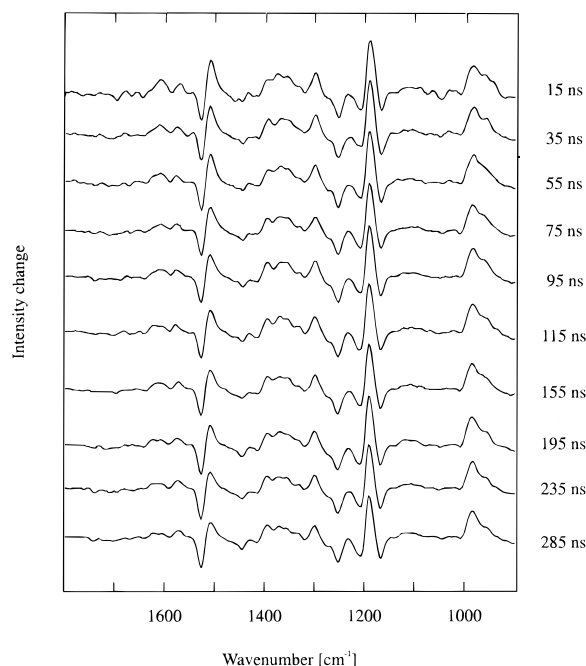


Figure 1. Time-resolved FTIR difference spectra measured at 25 °C at the indicated delay times after photolysis. The spacing of the original measurements was 10 ns; these spectra were averaged pairwise for the abbreviated data presentation here. The measured single-beam intensity changes are shown, with multiplication by (-1) to facilitate comparison with the absorption data in subsequent figures. The vertical scales of the 10 plotted spectra were normalized at 1208 cm^{-1} to partly compensate for a complex nonlinear instrumental rise time. The similarity of the spectral changes occurring during the first 50–100 ns after photolysis at 25 °C (e.g., the increase in the ratio of amplitudes at 983 and 956 cm^{-1} in this figure) to those seen at 5 °C on a 10-fold slower time scale (Figure 2) allows us to estimate an approximately 10-fold increase in τ_1 between 25 and 5 °C.

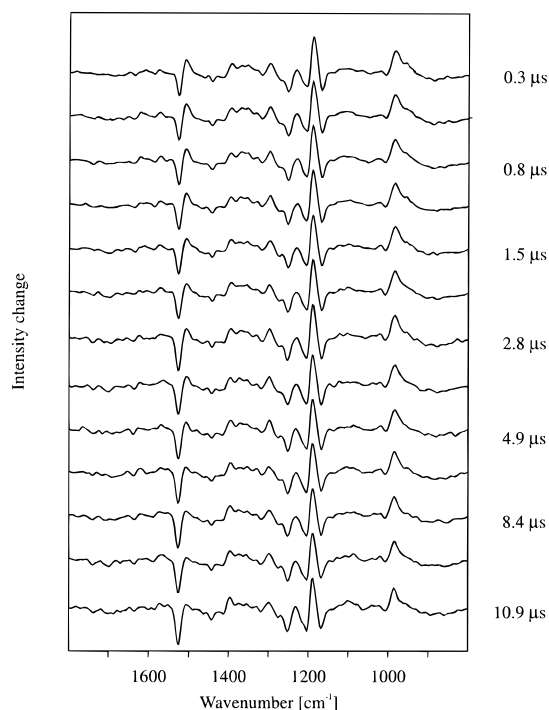


Figure 2. Time-resolved FTIR single-beam spectra measured at 5 °C with 50 ns spacing between time slices. Measured intensity changes are plotted as in Figure 1.

resolved microsecond absorption studies (sometimes described as the faster component of the $L \rightarrow M$ transition).^{4,10,11,28,47} Our

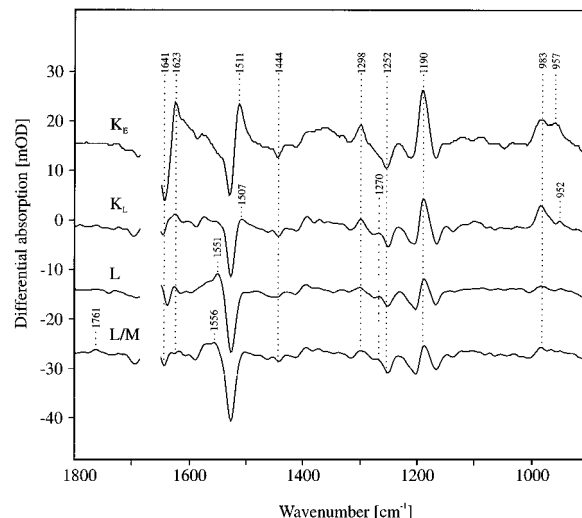


Figure 3. Time-resolved FTIR spectra of early intermediates of the bacteriorhodopsin photocycle at 25 °C. These spectra were obtained in two separate experiments and are not exactly scaled. The K_E spectrum was measured with 10 ns between the time slices and is presented as an average of the two first time slices (i.e., during the first 20 ns) after the excitation flash. The spectra of K_L , L , and the L/M mixture were obtained by global multiexponential fit of data measured with 100 ns time resolution in the range 0.3–70 μs after excitation.

$\tau_3 = 16 \pm 4 \mu\text{s}$ at 25 °C is in accord with published values of 21^{10} and $17\text{--}20 \mu\text{s}$ ⁴⁷ for this step.

Likewise, our observed τ_2 process corresponds to the decay of the K state as originally defined by Lozier et al.³ (We shall henceforth denote this K state³ as K_L —“late K ”—to distinguish it from its predecessor which we shall denote K_E —“early K ”. The $K_E \rightarrow K_L$ relaxation is the process described by τ_1 and will be discussed below.) The $K_L \rightarrow L$ transition has been studied extensively using time-resolved visible spectroscopy.^{3,4,10–13,28,47} Our value of $\tau_2 = 0.8 \pm 0.2 \mu\text{s}$ at 25 °C corresponds to the previously published values of 0.85^{10} or $0.78\text{--}0.80 \mu\text{s}$,⁴⁷ and our $\tau_2 = 7 \pm 2 \mu\text{s}$ at 5 °C corresponds to the previously published value of $5.5 \mu\text{s}$.¹⁰ The $K_L \rightarrow L$ process is believed to be practically unidirectional,^{4,6} the time constant for the reverse $L \rightarrow K_L$ transition being nearly 100 times longer than the forward one.⁴

The $K_E \rightarrow K_L$ relaxation processes ($\tau_1 = 640 \pm 90$ ns at 5 °C) has not previously been characterized (for details see below). At 25 °C the apparent time constant for the $K_E \rightarrow K_L$ transition (τ_1) is $\sim 5\text{--}10$ times shorter than at 5 °C.

Calculation of Intermediates' Spectra. Figures 3 and 4 present calculated difference spectra of the kinetically distinct intermediates detected on time scale 10 ns–50 μs at 25 and 5 °C, respectively. We consider these in reverse order of appearance in the photocycle. The latest (fourth) photointermediate spectrum (corresponding to a mixture of L and M states) was calculated from data at 25 °C by extrapolating all three of the observed exponential decay processes observed in the time range $<50 \mu\text{s}$ to their completion. The third spectrum (L state) was obtained by calculating what would be observed if the τ_3 process had not begun, but the τ_1 and τ_2 processes were nonetheless complete. The second (K_L) and the first (K_E) spectra were calculated in a similar fashion, by mathematically blocking the τ_2 and τ_1 processes sequentially.

The approach used to recalculate the K_E spectrum at 5 °C cannot be used at 25 °C, because at the higher temperature the τ_1 process cannot accurately be deconvoluted from the instrumental rise. Nevertheless, a practically pure (but unnormalized) K_E difference spectrum was obtained at 25 °C. This is because

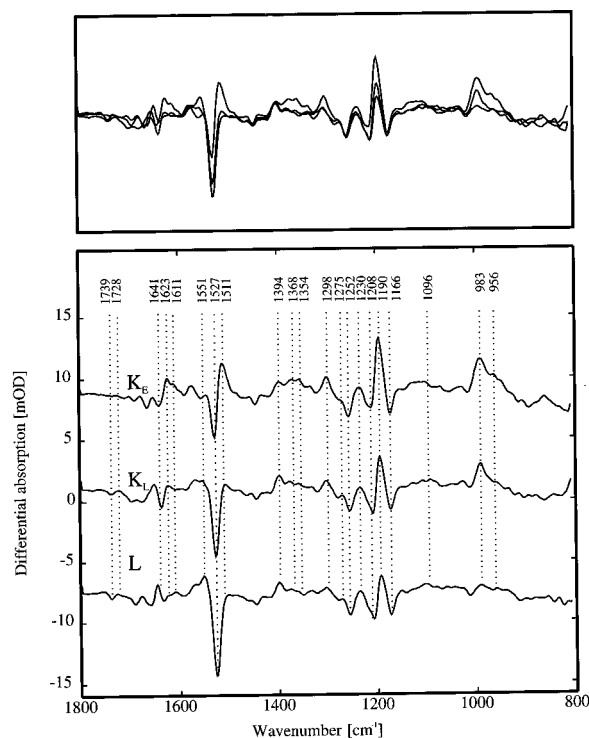


Figure 4. Time-resolved FTIR spectra of the early intermediates of the bacteriorhodopsin photocycle at 5 °C. The spectra of K_E , K_L , and L intermediates were obtained by a global multiexponential fit of data measured with 50 ns time resolution in the range 0.3–50 μ s after excitation. The top panel is a superposition to facilitate direct comparison. In the bottom panel, spectra are vertically displaced to allow a clearer view of individual intermediates.

the contribution of K_L (and L) to the measured difference spectra during the first 20 ns after photolysis is negligible, since $\tau_2 = 0.8 \pm 0.2 \mu$ s. That is, the unfitted difference spectrum of the first 20 ns after photolysis at 25 °C (see Figure 3) should correspond closely to the K_E difference spectrum obtained by kinetic fitting at 5 °C (Figure 4). The fact that it does provides a clear indication that there are no intermediates besides K_E in this time range.

The fitted τ_3 is an apparent rather than intrinsic time constant of the reversible $L \leftrightarrow M$ transition.^{4,6} Therefore, our spectrum obtained by extrapolating to completion of the $\tau_3 = 16 \mu$ s decay (Figure 3) corresponds to a mixture of L and M states.

The main features of the time-resolved difference spectra of the L/M mixture (in Figure 3) and of the L state (in Figures 3 and 4) are in accord with previously published spectra of M and L states obtained by a variety of methods.^{21,22,42,46,51–54} Our difference spectrum of the L/M mixture (Figure 3) shows a number of peaks reported earlier for M but not for L ; e.g., a carbonyl band of protonated Asp-85⁵⁶ at 1761 cm^{-1} and a positive peak in the ethylenic stretch region at 1556 cm^{-1} . The latter is clearly distinct from the peak observed at 1550 cm^{-1} in L .^{42,54} The minor differences between our spectrum of L at room temperature (Figures 3 and 4) and those of other authors^{42,54} are mostly due to our improved time resolution, which allow us to fully resolve the $L \rightarrow M$ transition (with an apparent time constant of $\tau_3 = 16 \pm 4 \mu$ s at 25 °C). Additional sources of discrepancy come from the fact that the $L \leftrightarrow M$ transition is reversible,^{4,6,57} and calculation of the L difference spectrum is highly dependent on assumed details of other kinetic decay pathways of L .

Unlike the $L \leftrightarrow M$ transition, the $K_L \rightarrow L$ transition is unidirectional.^{4,6} The K_L spectrum calculation is therefore unambiguous. The corresponding apparent time constant (τ_2

$= 7 \mu$ s at 5 °C and 0.8μ s at 25 °C) is equal to the intrinsic time constant of the $K_L \rightarrow L$ molecular process. This is the first time this process has been fully time resolved in vibrational spectroscopic studies, allowing us to correctly calculate the room temperature K_L IR difference spectrum. Our K_L spectrum displays distinct differences with earlier published K state spectra at low temperatures.^{17–22} We attribute this to real structural differences between the room-temperature K_L state and the frozen, i.e., not fully relaxed, conformation of the bathoproduct K trapped at low temperatures. Support for this interpretation comes from previous data indicating the presence of several distinct forms of K at cryogenic temperatures, which are observable under different preparation conditions.^{19,33}

There are no published data that could indicate whether the $K_E \rightarrow K_L$ decay is reversible or unidirectional. Therefore, we are unable to say whether the τ_1 time constant represents an intrinsic or an apparent time constant for the $K_E \rightarrow K_L$ process. If there is a significant reverse rate (i.e., $K_L \rightarrow K_E$), then $1/\tau_1$ represents the sum of the intrinsic rate constants for the forward ($K_E \rightarrow K_L$) and reverse ($K_L \rightarrow K_E$) reactions. Even if τ_1 is not an intrinsic time constant, its value allows us to make some useful conclusions. If the rate of the reverse ($K_L \rightarrow K_E$) transition is much higher than that of the forward one, the transient balance between the K_E and K_L intermediates would be shifted toward K_E . This would result in low concentrations of K_L , and the spectrum of K_L (calculated in Figure 4 under assumption of the absence of the reverse reaction) should be much smaller in amplitude than that of K_E . That is not the case, and therefore the rate of the reverse ($K_E \leftarrow K_L$) transition cannot be much higher than that of the forward one ($K_E \rightarrow K_L$). Thus, at room temperature either the $K_E \rightarrow K_L$ decay is approximately unidirectional or both the $K_E \rightarrow K_L$ and the $K_E \leftarrow K_L$ intrinsic transitions have nanosecond time constants.

For calculating the K_E state spectrum in Figure 4, we assumed that the $K_E \rightarrow K_L$ transition (with $\tau_1 = 640 \pm 90$ ns at 5 °C) is unidirectional. However, if this assumption is not true (i.e., the $K_E \leftrightarrow K_L$ transition is reversible), the calculated K_E spectrum in Figure 4 is a mixture of K_E and K_L states, and therefore the real differences between the K_E and K_L states would be more (rather than less) pronounced than in Figure 4. That is, the differences between the K_E and K_L states presented in Figure 4 are a “lower bound” on the true differences. The small differences between K_E spectrum in Figures 3 and 4 might be indicative of the possible presence of the reverse ($K_E \leftarrow K_L$) reaction.

Detailed Comparison of IR Spectra of K_E and K_L Intermediates. The existence of two distinct K species was suggested by previous time-resolved visible,^{12,37} resonance Raman,^{24,25,34,38} and IR^{22,29,41} spectroscopy data. However, errors in estimating the corresponding time constant led to erroneous calculation of photointermediate spectra in previous publications. Our K_E state is therefore a new intermediate detected and characterized in the bacteriorhodopsin photocycle. (See Discussion for details on its difference from K and K_L states as defined by Shichida et al.³⁷) Its IR spectrum has common features with K difference spectra measured at -196 °C ^{17–22} but differs from those distinctly.

The IR spectrum of K_E differs from the spectrum of its successor state, K_L , in several important regions throughout the mid-IR range. These differences are most pronounced in the following spectral ranges:

1640–1610 cm^{-1} Range. The main contribution to this region is expected from the protonated Schiff base $\text{C}=\text{NH}$ stretch vibration.^{18,59,60} Both the K_E and K_L intermediates have a characteristic positive peak at 1623 cm^{-1} and a negative peak

at around 1640 cm^{-1} . However, there is an additional positive peak at 1611 cm^{-1} in the K_E state. The amplitude of the 1623 cm^{-1} peak is greatly decreased during transition to K_L , and the peak at 1611 cm^{-1} is decreased even further, to form a shoulder. These changes could indicate weakening of the Schiff base hydrogen bond and/or a strained (nonrelaxed) configuration of the Schiff base in K_E which relaxes during the $K_E \rightarrow K_L$ and $K_L \rightarrow L$ decays. This is reflected in successive intensity decreases of the 1623 cm^{-1} peak during these transitions.

1554–1506 cm^{-1} Range. This is the region of the chromophore ethylenic ($\text{C}=\text{C}$) stretch vibrations, as well as of the amide II vibrations of the peptide backbone. The main feature in the IR spectra in this region—an intense negative peak at 1527 cm^{-1} due to depletion of the bR_{568} state—is present in all difference spectra of the photocycle intermediates. Its apparent amplitude is practically the same in both K_E and K_L states but is increased upon L state formation. The 1527 cm^{-1} negative peak originates from shifts in the frequency of the chromophore's $\text{C}=\text{C}$ stretch in the photoproducts,^{24,25,61} as further indicated by the appearance of positive peaks at adjacent frequencies. Appearance of a positive peak at higher frequencies (e.g., at $1556\text{--}1557\text{ cm}^{-1}$ in the M state^{42,54}) is usually associated with a blue shift in absorption of the corresponding intermediate, while a prominent positive peak at lower frequencies (e.g., in the region $1509\text{--}1514\text{ cm}^{-1}$ in the low-temperature K state^{18,22}) indicates a red-shifted intermediate.

The K_E state has a big positive peak at 1511 cm^{-1} , which is decreased in size and shifted to 1506 cm^{-1} upon K_L formation. This large change of the ethylenic region in the IR is surprising, in view of the fact that room temperature submicrosecond^{10,11,47} and nanosecond^{12,13,39} visible spectroscopies fail to detect any significant changes in the visible absorption in the nanosecond time range (i.e., during the $K_E \rightarrow K_L$ transition). The downshifted ethylenic peak at 1506 cm^{-1} (K_L) disappears completely upon L state formation, while an upshifted peak at 1551 cm^{-1} appears, clearly indicating the blue-shifted visible absorption maximum of the L state.

1410–1280 cm^{-1} Range. Vibrations in this range are dominated by in-plane hydrogen bending or rocking modes, with contributions from $\text{C}-\text{C}$ and $\text{C}-\text{CH}_3$ stretches.⁶² There are two large positive difference peaks: at 1394 cm^{-1} and a broad band between 1380 and 1280 cm^{-1} (with main peaks at 1368 , 1354 , and 1298 cm^{-1} ; see Figure 4) in K_E . The latter loses most of its intensity upon decay to K_L while the 1394 cm^{-1} is practically unaffected by the $K_E \rightarrow K_L$ transition (Figure 4). Bands in this region in K_E are likely to be due at least in part to hydrogen in-plane rocking vibrations of the retinylidene chromophore, which are expected to dominate the early structural changes after the primary photoreaction. The 1354 cm^{-1} peak is probably due to the Schiff base ($\text{N}-\text{H}$) in-plane rock coupled to the $\text{C}_{15}-\text{H}$ rock, since a band at this frequency was shown to be sensitive to both C_{15} deuteration and to H/D exchange with solvent in submicrosecond time-resolved IR spectra of bacteriorhodopsin photocycle.²² Furthermore, a peak at 1348 cm^{-1} in the -196°C static difference spectrum of $\text{bR} \rightarrow \text{K}$ transition was also shown to be sensitive to the same set of isotopic substitutions.^{21,63,64} Likewise, the 1298 cm^{-1} peak most probably corresponds to a frequency of $\sim 1295\text{ cm}^{-1}$ observed in the low-temperature FTIR and resonance Raman spectra of K. The latter vibration was tentatively identified as arising from a mixed mode involving the $\text{C}_{10}-\text{H}$, $\text{C}_{11}-\text{H}$, and $\text{C}_{12}-\text{H}$ in-plane rocking vibrations of chromophore based on specific isotope labeling.⁶⁴ No specific assignment of the 1368 cm^{-1} peak is possible at this point. Loss of positive absorption in the $1410\text{--}1280\text{ cm}^{-1}$ region in the course of $K_E \rightarrow K_L$ transition

is consistent with a relaxation process in the chromophore, taking place at room temperature in the nanosecond time range.

1280–1260 cm^{-1} Range. A negative peak at 1275 cm^{-1} is first resolved in the K_L state; in K_E , there is at most a weak negative shoulder at this frequency. Previously, a negative peak at 1277 cm^{-1} in the low-temperature K state was attributed to the $\text{C}-\text{O}$ stretch vibration of a tyrosinate in unphotolyzed bR, which was hypothesized to become protonated during the K state formation at -196°C ²⁰ (see also ref 65). This peak was later assigned to Tyr-185.⁵² On the basis of this assignment, we tentatively propose that at room temperature Tyr-185 either gains a proton or is strongly perturbed during the $K_E \rightarrow K_L$ transition. This process takes place on a nanosecond time scale (i.e., after formation of the first K-like photoproduct, K_E), rather than on the picosecond scale as might have been expected from low-temperatures studies of the $\text{bR} \rightarrow \text{K}$ reaction.^{20,52,65} It is much easier to imagine a protonation (or any other perturbation involving a proton movement) taking place on a nanosecond, rather than picosecond, time scale. Thus, the K state trapped at cryogenic temperatures could represent a hybrid of the K_E and K_L structures, in which some of the large-scale conformational relaxations are blocked.

1260–1150 cm^{-1} Range. Distinct changes between K_E and K_L states take place in the chromophore fingerprint region. This region of the K_E IR difference spectrum is dominated by two groups of peaks: (i) a combination of a large positive peak at 1190 cm^{-1} and two large negative peaks at 1166 and 1208 cm^{-1} ; (ii) a positive/negative difference band at $1230/1252\text{ cm}^{-1}$. Both sets of peaks are thought to arise from shifts in $\text{C}-\text{C}$ stretch vibrations of the retinylidene-lysine group. However, hydrogen in-plane rocking vibrations also make strong contributions to the normal modes in this region.⁶² During the $K_E \rightarrow K_L$ transition, both positive peaks (at 1190 and 1230 cm^{-1}) decrease in amplitude. The 1190 cm^{-1} peak undergoes a slight upshift in frequency, which is reflected in a simultaneous decrease in intensity of the positive difference peak around 1190 cm^{-1} and the negative one around 1166 cm^{-1} and an increase in the negative absorption around 1208 cm^{-1} . This is accompanied by shifts in apparent positions of the corresponding peaks by $1\text{--}4\text{ cm}^{-1}$. These changes are further evidence of relaxation processes in and around retinal chromophore in the nanosecond time domain.

1140–1070 cm^{-1} Range. K_E , but not K_L , shows a broad positive band in this region. This is apparently a superposition of several closely spaced bands, not resolved in our experiments. The origin of these features, which are very reproducible, is as yet not clear. However, this broad band disappears in K_L , providing additional evidence for a specific nanosecond conformational relaxation.

1000–900 cm^{-1} Range. A major change in the nanosecond time domain takes place in the region of retinal chromophore hydrogen out-of-plane (HOOP) wag vibrations (see also refs 22, 29, 40, and 41). Strong IR absorption in this region was reported for the K state trapped at cryogenic temperatures.^{17,18,20,22} In our room temperature spectra of K_E and K_L (Figure 4) the main features in this region are the two positive peaks around 983 and 956 cm^{-1} (see also refs 22, 40, and 41). At 8 cm^{-1} resolution, our K_E spectra do not show whether a third peak might be present corresponding to the 974 cm^{-1} reported for K at -196°C .¹⁸ In earlier IR nanosecond studies,^{40,41} the positive peak at around 984 cm^{-1} was attributed to a "late K", while that at 955 cm^{-1} to the "early K". Our results contradict this simple assignment: in our spectra these two peaks are present in both K_E and K_L intermediates. Amplitudes of both of these peaks are decreased during the K_E

$\rightarrow K_L$ transition, while the ratio of their amplitudes ($\Delta A_{983}/\Delta A_{956}$) increases.

The strong IR absorbance intensity in the HOOP frequency region in K_E is the most direct indication that the retinal chromophore in this species is in a twisted, nonrelaxed conformation. The strongest peak in both K_E and K_L HOOP region at 983 cm^{-1} can be tentatively assigned to the $C_{15}\text{--H}$ HOOP.²² The $K_E \rightarrow K_L$ transition results in a decrease of HOOP intensities, clearly indicating that a major conformational relaxation near the Schiff base group of retinal take place on a nanosecond time scale.

Discussion

We have characterized kinetically and spectrally a transition between two K-like states in the bacteriorhodopsin photocycle with a time constant $\tau_1 = 640 \pm 90\text{ ns}$ at 5°C . This transition is distinct from the later well-known $K_L \rightarrow L$ transition ($\tau_2 = 7 \pm 2\text{ }\mu\text{s}$ at 5°C ; $\tau_2 = 0.8 \pm 0.2\text{ }\mu\text{s}$ at 25°C).

Our τ_1 ($K_E \rightarrow K_L$) transition does not correspond well with previously published data on nanosecond transitions of bacteriorhodopsin. Shichida et al.³⁷ saw a visible spectral change between 0.5 and 150 ns after photolysis and concluded that this could be explained only by introducing a new "KL" intermediate. However, they made no measurements at intermediate times and were therefore unable to estimate a time constant (although subsequently other workers^{12,13,22,39,41} estimated a time constant of $\sim 10\text{ ns}$ from raw data of Shichida et al.³⁷). The conclusions of Shichida et al.³⁷ were based on a miscalculation: they assumed that the 0.5 ns difference spectrum corresponds to 100% of K_E ("K" in their notation) and the 150 ns spectrum corresponds to a mixture of 93.4% of K_L ("KL" in their notation) and 6.6% of L. In reality, 150 ns after the excitation flash, $\sim 12\%$ of the excited chromophores (rather than 6.6% as assumed by ref 37) are already in the L state,^{10,12,13} and the rest are distributed between K_E and K_L . That is, the contribution of L to the 150 ns difference spectrum was underestimated, and the contribution of K_E was neglected, leading to an erroneously calculated spectrum of the KL state³⁷ and misleading evidence for a time constant of $\sim 10\text{ ns}$ for the $K_E \rightarrow K_L$ transition.

Introduction of the KL state³⁷ caused confusion in the nomenclature of the bacteriorhodopsin intermediates. The K state as originally defined by Lozier et al.³ was renamed as KL, while the traditional term "K" was reassigned to a precursor state that had supposedly been detected as decaying into KL on a nanosecond time scale.³⁷ It took 10 years and publications by several groups^{12,13,39} to prove that there is no visible spectral distinction between the intermediates identified as "K" and "KL". In fact, there seems to be no kinetic process detectable in the visible in the nanosecond time range.^{13,39}

Thus, our $K_E \rightarrow K_L$ transition has no kinetic correspondence to any process described previously by visible time-resolved studies.^{4,9–13,28,37,39} Our discovery of the new K_E intermediate, and its full kinetic characterization, have allowed us to characterize it spectrally and to distinguish it from K_L , which is actually the K state as originally defined.³

We are not the first to measure kinetic IR difference spectra of bacteriorhodopsin on the nanosecond time scale (see refs 22, 29, 40, and 41). While there is a good consensus between our raw data and those previously published, some of our conclusions are in contradiction with previous studies.^{22,41} For instance, excellent room-temperature IR spectra at 0.7 and 8 μs after excitation were published previously by Weidlich and Siebert²² without kinetic decomposition. Instead, a $\sim 10\text{ ns}$ time constant for the $K \rightarrow KL$ transition was assumed based on prior

visible spectroscopy data.³⁷ As a result, both the spectrum at 0.7 μs (which is a mixture of K_E , K_L , and L states) and that at 8 μs (which is a mixture of L and M) were interpreted as different mixtures of KL and L.²² Our raw spectra at 0.7 and 8 μs are practically indistinguishable from those of Weidlich and Siebert.²² However, unlike those earlier workers, we did not limit our spectral calculations to sums and differences of spectra measured at two or three particular time delays, but rather based them on a global fit of the whole time range from 10 ns to 50 μs after excitation. Thus, we reached somewhat different conclusions. Nevertheless, the similarity of our raw spectra at two particular delay times (0.7 and 8 μs) with the corresponding time slices in previously published data²² produces independent confirmation for spectra reported here.

Sasaki et al.⁴¹ (see also refs 29 and 40) also obtained nanosecond IR difference spectra of the bacteriorhodopsin photocycle, but with a poorer signal-to-noise ratio and more limited spectral range. This prevents us from detailed comparison of their and our raw data in any but the strongest peaks. These peaks match each other well, despite the fact that they were taken using a somewhat different IR spectroscopic approach.

In addition to the IR data mentioned above (which are directly comparable to our raw data), we can correlate our spectra with results obtained by low-temperature and time-resolved resonance Raman (TR³) spectroscopy, which is restricted to detection of chromophore vibrations. In fact, distinct differences between K-like photoproducts measured at room and low temperatures were first noted by time-resolved RR methods.^{24,25,27,34,38,66} These differences were observed throughout the spectrum, i.e., in ethylenic, fingerprint, and HOOP regions. Changes in RR intensity in the HOOP region in various K-like states provide direct information on torsional distortions of the chromophore during the early stages of the photocycle. The most detailed RR kinetic study (for the time range 2.8 ps–13.5 ns at 10°C) was published by Doig et al.,²⁷ who noted that unusually high RR intensities in the HOOP region are present already in the J state. These unusually large HOOP intensities initially decrease during the first $\sim 3\text{ ps}$ of J relaxation but are later restored with a 10–40 ps time constant.²⁷ This indicates a complex pattern of the onset of the torsional disturbances in the chromophore conformation.

Time-resolved RR spectra measured with delays of 40 ps, 15 ns, 100 ns,^{24,25} and 60 ns^{34,38} after excitation revealed HOOP peaks at 811, 960–971, and 984–991 cm^{-1} . Particular RR frequencies in the HOOP region are expected to have fairly close correspondence to those measured with IR absorption. However, relative intensities of the overlapping HOOP peaks are not expected to match in RR and FTIR difference spectra. As a result, one cannot expect an exact correspondence between RR and FTIR peak maxima. RR spectra measured with nanosecond^{24,25,34,38} or picosecond time resolution^{24,25,27,66} exhibit distinct differences, even between similarly measured spectra reported by different groups. Thus, it is difficult to draw firm conclusions about the frequency shifts of our K_E and K_L peaks relative to the RR bands reported previously.

In the L state, the intensity of the HOOP bands is decreased, as detected by both resonance Raman scattering^{25,61,68} and IR absorption^{22,42,53} (see also Figures 3 and 4). However, no attempts were ever made with the RR technique to measure kinetics of the HOOP band disappearance, and the maximal time delays used in most time-resolved RR studies of K intermediate were limited to tens of nanoseconds.

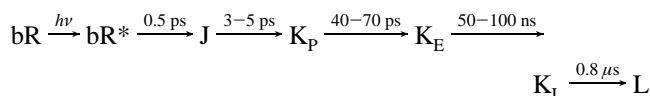
Comparison of IR data of the HOOP absorption bands in our K_E data (at 956 and 983 cm^{-1}) with the intense HOOP mode

IR absorption reported for the low-temperature K state (at 956, 974, and 984 cm^{-1})^{18,22} indicates that the twisted conformation of retinal does not relax prior to K_E decay. The total intensity in the 950–990 cm^{-1} HOOP modes of the K_E is similar to, or larger than, that observed in the low-temperature K state.²² This indicates that the torsional deformations present a few nanoseconds after the photolysis at room temperature are as large as those that can be trapped in a rigid frozen protein.

The time course of IR absorption changes in Figures 1 and 2 (which were also used to calculate the spectra in Figures 3 and 4) was obtained with nearly saturating excitation energy density (10–12 mJ/cm^2). This level of excitation produces some irreversible photobleaching (which is especially evident with higher energy densities, e.g., >20 mJ/cm^2 ^{48,69}) as well as the possibility of transient secondary photoproducts. Earlier, the yield per flash for irreversible bleaching was estimated to be 2×10^{-4} for 34 mJ/cm^2 flashes.⁴⁸ These photoproducts arise from two-quantum absorption; their yield is thus proportional to the square of excitation energy density.⁶⁹ On the other hand, a single nearly saturating nanosecond flash at 532 nm yields ~40% photoconversion into the normal photocycle.⁷⁰ On the basis of these values, we estimate that under our experimental conditions a single-flash excitation is expected to yield native intermediates and irreversibly photobleached products in the ratio ~20000:1. That is, contributions from “non-native” photoproducts under our measuring conditions are expected to be ~400 times below the experimental noise level. The irreversible photobleaching^{47,48,69} results from accumulation of two states: a stable UV-absorbing state^{48,69} and a 605 nm-absorbing species which is present only during early stages of photobleaching.⁶⁹ The former has no evident absorption at 532 nm,^{48,69} while the latter has at least 4 times lower extinction at 532 nm than unphotolyzed bacteriorhodopsin.⁴⁸ On the basis of this, we estimate that any contributions from secondary photoproducts of these photobleached species should be below 10% of the measured difference spectra. That is, the amplitudes of the peaks attributed by us to K_E and K_L are incompatible with an assumption that they are coming from species formed in parallel to the native photocycle.

To test these assumptions, we performed additional experiments with 3-fold reduced excitation energy (~4 mJ/cm^2 , data not shown). This 3-fold reduction in excitation eliminated any obvious irreversible photobleaching, as a result of the ~9-fold reduction in the probability of two-photon processes. Subsequent multiexponential analysis yielded results fully consistent with those obtained at ~12 mJ/cm^2 . That is, the kinetics and calculated spectra of the K_E and the K_L intermediates are not significantly affected by this variation in excitation energy density. Therefore, both the K_E and the K_L states are intermediates of the native photocycle of bacteriorhodopsin, and their presence cannot be assigned to any secondary photochemistry or two-photon process.

Combining our kinetic data with those previously published,^{7,8,27} we obtain the following sequence of intermediates in the early stages of the bacteriorhodopsin photocycle at room temperature:



A 40–70 ps transition between a primary K-like state (K_p) and a subsequent K-like state (which we assume to be identical with the K_E state we have measured) was introduced by Doig et al.,²⁷ but has not been confirmed. Therefore, the existence of an

additional kinetically distinct intermediate, K_p , between J and our K_E is not yet fully established.

Creation of the K state in the bacteriorhodopsin photocycle has been associated with completion of the primary charge separation.⁷¹ The photocycle is initiated by a visible quantum absorbed by the electronic subsystem of the chromophore. That is, the K state is formed before the stored excitation energy is transferred from the electronic subsystem of retinal to the protonic subsystem and/or protein environment. The widely accepted mechanism for K state formation is an *all-trans* to *13-cis* isomerization of the retinal chromophore.^{72,73} An alternative hypothesis⁷⁴ attributed this step to electronic charge separation *inside* retinal.

The time constant for K state formation is shorter than ~50 ps both at –196 and at –271 °C.^{23,75} The ~50 ps time constant at –271 °C should not present a problem for a full double-bond isomerization, if it were to take place in a vacuumlike environment, but is several orders of magnitude too fast for a solventlike environment.^{76–78} Retinal isomerization inside a protein in the bacteriorhodopsin photocycle takes place in an environment intermediate between solvent and vacuum. That is, electrostatic interactions of the positively charged Schiff base with amino acid side chains might create some dissipative forces similar to a solventlike environment. This should most probably result in incomplete isomerization (a twisted conformation) at cryogenic temperatures⁶³ and/or on the picosecond time scale,^{24,25} with further structural relaxation of *retinal* at later times or upon unfreezing.

Our results support the idea that retinal isomerization is not a simple, one-step process. Instead, it starts with bond energy redistribution inside retinal during the first femtoseconds after excitation and is completely finished only on the nanosecond time scale at physiological temperatures. That is, the $K_E \rightarrow K_L$ and $K_L \rightarrow L$ transitions are the final steps of retinal relaxation in the course of its *all-trans* to *13-cis* isomerization. In the K_E state (formed on the picosecond time scale), the retinylidene chromophore is highly perturbed and subject to major twisting deformations. It is during the nanosecond relaxation of K_E to K_L that the energy stored in the chromophore starts to be transferred into the successive perturbations of the Schiff base environment. Most of the IR spectral differences between K_E and K_L appear to involve the Schiff base end of the chromophore. The $K_E \rightarrow K_L$ relaxation therefore probably involves qualitatively similar structural changes as were hypothesized for a K-state relaxation thought to occur on a ~10-fold faster time scale.⁴¹ On the other hand, at cryogenic temperatures, the retinal seems to be frozen in a twisted, i.e., incompletely relaxed, structure (as proposed earlier⁶³), resulting in a low-temperature K state which cannot be directly identified with either the K_E or K_L intermediate of the native photocycle at room temperature.

Acknowledgment. This work was supported by Fogarty International Fellowship 1-F05-TW05212-1 (to A.K.D.) and by NIH Grant GM46854 (to M.S.B.). The Bruker IFS-66 step-scan FTIR spectrometer was obtained with NIH shared instrumentation Grant S10 RR08959. We are grateful to Dr. Susan E. Plunkett for extensive assistance with setting up the step-scan FTIR measurements.

Note Added in Proof. While our manuscript was under consideration, a paper reporting similar experiments was published (Frei et al. *J. Phys. Chem.* **1996**, *100*, 16026–16033). The raw data in that work is mostly consistent with data reported here, but there are distinct differences in interpretation. These differences are mostly due to our more extensive kinetic analysis, which allowed us to extract additional information,

including the distinction and characterization of the K_E and K_L intermediates.

References and Notes

- (1) Stoeckenius, W.; Lozier, R. H.; Bogomolni, R. A. *Biochim. Biophys. Acta* **1979**, *505*, 215.
- (2) Lanyi, J. K. *Biochim. Biophys. Acta* **1993**, *1183*, 241.
- (3) Lozier, R. H.; Bogomolni, R. A.; Stoeckenius, W. *Biophys. J.* **1975**, *15*, 955.
- (4) Lozier, R. H.; Xie, A.; Hofrichter, J.; Clore, G. M. *Proc. Natl. Acad. Sci. U.S.A.* **1992**, *89*, 3610.
- (5) Dinur, U.; Honig, B.; Ottolenghi, M. *Photochem. Photobiol.* **1981**, *33*, 523.
- (6) Váró, Gy.; Lanyi, J. K. *Biochemistry* **1991**, *30*, 5016.
- (7) Sharkov, A. V.; Pakulev, A. V.; Chekalin, S. V.; Matveetz, Y. A. *Biochim. Biophys. Acta* **1985**, *808*, 94.
- (8) Polland, H.-J.; Franz, M. A.; Zinth, W.; Kaiser, W.; Kolling, E.; Oesterheld, D. *Biophys. J.* **1986**, *49*, 651.
- (9) Nagle, J. F.; Parodi, L. A.; Lozier, R. H. *Biophys. J.* **1982**, *38*, 161.
- (10) Xie, A. H.; Nagle, J. F.; Lozier, R. H. *Biophys. J.* **1987**, *51*, 627.
- (11) Maurer, R.; Vogel, J.; Schneider, S. *Photochem. Photobiol.* **1987**, *46*, 247.
- (12) Milder, S. J.; Kliger, D. S. *Biophys. J.* **1988**, *53*, 465.
- (13) Yamamoto, N.; Ebbesen, T. W.; Ohtani, H. *Chem. Phys. Lett.* **1994**, *228*, 61.
- (14) Stoeckenius, W.; Lozier, R. H. *J. Supramol. Struct.* **1974**, *2*, 769.
- (15) Hurley, J. B.; Ebrey, T. G.; Honig, B.; Ottolenghi, M. *Nature* **1977**, *270*, 540.
- (16) Braiman, M. S.; Mathies, R. *Biochemistry* **1980**, *19*, 5421.
- (17) Rothschild, K. J.; Marrero, H. *Proc. Natl. Acad. Sci. U.S.A.* **1982**, *79*, 4045.
- (18) Rothschild, K. J.; Marrero, H.; Braiman, M. S.; Mathies, R. *Photochem. Photobiol.* **1984**, *40*, 675.
- (19) Rothschild, K. J.; Roepe, P.; Gillespie, J. *Biochim. Biophys. Acta* **1985**, *808*, 140.
- (20) Rothschild, K. J.; Roepe, P.; Ahl, P.; Earnest, T. N.; Bogomolni, R. A.; Das Gupta, S. K.; Mulliken, C. M.; Herzfeld, J. *Proc. Natl. Acad. Sci. U.S.A.* **1986**, *83*, 347.
- (21) Siebert, F.; Mänte, W. *Eur. J. Biochem.* **1983**, *130*, 565.
- (22) Weidlich, O.; Siebert, F. *Appl. Spectrosc.* **1993**, *47*, 1394.
- (23) Applebury, M. L.; Peters, K. S.; Rentzepis, P. M. *Biophys. J.* **1978**, *23*, 375.
- (24) Hsieh, C.-L.; El-Sayed, M. A.; Nicol, M.; Nagumo, M.; Lee, J.-H. *Photochem. Photobiol.* **1983**, *38*, 83.
- (25) Hsieh, C. L.; Nagumo, M.; Nicol, M.; El-Sayed, M. A. *J. Phys. Chem.* **1981**, *85*, 2714.
- (26) Stern, D.; Mathies, R. *Springer Proc. Phys.* **1985**, *4*, 250.
- (27) Doig, S. J.; Reid, P. J.; Mathies, R. A. *J. Phys. Chem.* **1991**, *95*, 6372.
- (28) Maurer, R.; Vogel, J.; Schneider, S. *Photochem. Photobiol.* **1987**, *46*, 255.
- (29) Sasaki, J.; Maeda, A.; Kato, C.; Hamaguchi, H. *Biochemistry* **1993**, *32*, 867.
- (30) Mao, B. *Photochem. Photobiol.* **1981**, *33*, 407.
- (31) Kalisky, O.; Ottolenghi, M. *Photochem. Photobiol.* **1982**, *35*, 109.
- (32) Kuschmitz, D.; Hess, B. *FEBS Lett.* **1982**, *138*, 137.
- (33) Balashov, S. P.; Karneyeva, N. V.; Litvin, F. F.; Ebrey, T. G. *Photochem. Photobiol.* **1991**, *54*, 949.
- (34) Braiman, M. S. *Methods Enzymol.* **1986**, *127*, 587–597.
- (35) Braiman, M. S.; Mathies, R. *Biophys. J.* **1983**, *41*, 14a.
- (36) Dioumaev, A. K.; Keszthelyi, L. *Acta Biochim. Biophys. Hung.* **1988**, *23*, 271.
- (37) Shichida, Y.; Matuoka, S.; Hidaka, Y.; Yoshizawa, T. *Biochim. Biophys. Acta* **1983**, *723*, 240.
- (38) Smith, S. O.; Braiman, M. S.; Mathies, R. In *Time-Resolved Vibrational Spectroscopy*; Atkinson, G. H., Ed.; Academic Press: New York, 1983; pp 219–230.
- (39) Delaney, J. K.; Brack, T. L.; Atkinson, G. H. *Biophys. J.* **1993**, *64*, 1512.
- (40) Yuzawa, T.; Kato, C.; George, M. W.; Hamaguchi, H. *Appl. Spectrosc.* **1994**, *48*, 684.
- (41) Sasaki, J.; Yuzawa, T.; Kandori, H.; Maeda, A.; Hamaguchi, H. *Biophys. J.* **1995**, *68*, 2073.
- (42) Hessling, B.; Souvignier, G.; Gerwert, K. *Biophys. J.* **1993**, *65*, 1929.
- (43) Hwang, S. B.; Korenbrot, J. I.; Stoeckenius, W. *Biochim. Biophys. Acta* **1978**, *509*, 300.
- (44) Kalisky, O.; Ottolenghi, M.; Honig, B.; Korenstein, R. *Biochemistry* **1981**, *20*, 649.
- (45) Oesterheld, D.; Stoeckenius, W. *Methods Enzymol.* **1974**, *31*, 667.
- (46) Braiman, M. S.; Ahl, P. L.; Rothschild, K. J. *Proc. Natl. Acad. Sci. U.S.A.* **1987**, *84*, 5221.
- (47) Hofrichter, J.; Henry, E. R.; Lozier, R. H. *Biophys. J.* **1989**, *56*, 693.
- (48) Govindjee, R.; Balashov, S. P.; Ebrey, T. G. *Biophys. J.* **1990**, *58*, 597.
- (49) Sharonov, A. Y.; Tkachenko, N. V.; Savransky, V. V.; Dioumaev, A. K. *Photochem. Photobiol.* **1991**, *54*, 889.
- (50) Bevington, P. R.; Robinson, D. K. *Data Reduction and Error Analysis for the Physical Sciences*, 2nd ed; McGraw-Hill: New York, 1992; Chapter 11.
- (51) Roepe, P.; Ahl, P. L.; Das Gupta, S. K.; Herzfeld, J.; Rothschild, K. J. *Biochemistry* **1987**, *26*, 6696.
- (52) Braiman, M. S.; Mogi, T.; Stern, L. J.; Hackett, N. R.; Chao, B.; Khorana, H. G.; Rothschild, K. J. *Proteins: Struct., Funct., Genet.* **1988**, *3*, 219.
- (53) Braiman, M. S.; Bousché, O.; Rothschild, K. J. *Proc. Natl. Acad. Sci. U.S.A.* **1991**, *88*, 2388.
- (54) Chen, W.-G.; Braiman, M. S. *Photochem. Photobiol.* **1991**, *54*, 905.
- (55) There are, however, small but reproducible differences between static IR difference spectra of L and M intermediates trapped at low temperature^{22,46,51,52} and the corresponding room-temperature time-resolved spectra.^{22,42,53,54} These are probably due to inadequacies in the isolation of pure intermediates in low-temperature trapped mixtures.
- (56) Braiman, M. S.; Mogi, T.; Marti, T.; Stern, L. J.; Khorana, H. G.; Rothschild, K. J. *Biochemistry* **1988**, *27*, 8516.
- (57) Váró, Gy.; Lanyi, J. K. *Biochemistry* **1990**, *29*, 2241.
- (58) If the rate for the reverse ($K_L \rightarrow K_E$) transition is much lower than that of the forward one, we can disregard it and consider the K_E to K_L transition as unidirectional.
- (59) Braiman, M. S.; Rothschild, K. J. *Annu. Rev. Biophys. Biophys. Chem.* **1988**, *17*, 541.
- (60) Fodor, S. P. A.; Ames, J. B.; Gebhard, R.; Van den Berg, E. M. M.; Stoeckenius, W.; Lugtenburg, J.; Mathies, R. A. *Biochemistry* **1988**, *27*, 7097.
- (61) Smith, S. O.; Lugtenburg, J.; Mathies, R. A. *J. Membr. Biol.* **1985**, *85*, 95.
- (62) Smith, S. O.; Myers, A. B.; Mathies, R. A.; Pardo, J. A.; Winkel, C.; Van den Berg, E.; Lugtenburg, J. *Biophys. J.* **1985**, *47*, 653.
- (63) Braiman, M. S.; Mathies, R. *Proc. Natl. Acad. Sci. U.S.A.* **1982**, *79*, 403.
- (64) Braiman, M. S. Structural Changes of the Bacteriorhodopsin Chromophore during its Proton-Pumping Photocycle. Ph.D. Dissertation, University of California, Berkeley, 1983; pp 1–261.
- (65) Lin, S.-L.; Ormos, P.; Eisenstein, L.; Govindjee, R.; Konno, K.; Nakanishi, K. *Biochemistry* **1987**, *26*, 8327.
- (66) Brack, T. L.; Atkinson, G. H. *J. Mol. Struct.* **1989**, *214*, 289.
- (67) A kinetic process with a similar time constant (40–100 ps) was detected in ethylenic region²⁷ which seems to account for the previously described discrepancies between time-resolved RR data measured with nano- and picosecond time resolution.^{24,25,35}
- (68) Lohrmann, R.; Stockburger, M. *J. Raman Spectrosc.* **1992**, *23*, 575.
- (69) Chizhov, I. V.; Engelhard, M.; Sharkov, A. V.; Hess, B. In *Structure and Function of Retinal Proteins*; Rigaud, J. L., Ed.; Colloque INSERM Vol. 221; John Libbey Eurotext: Paris, 1992; pp 171–173.
- (70) Dioumaev, A. K.; Savransky, V. V.; Tkachenko, N. V.; Chukharev, V. I. *J. Photochem. Photobiol. B* **1989**, *3*, 397.
- (71) Birge, R. R. *Biochim. Biophys. Acta* **1990**, *1016*, 293.
- (72) Oesterheld, D. *Agnew. Chem., Int. Ed. Engl.* **1976**, *15*, 17.
- (73) Ottolenghi, M. *Adv. Photochem.* **1980**, *12*, 97.
- (74) Chernavskii, D. S. *Biophysics* **1994**, *39*, 651.
- (75) Kaufmann, K. J.; Sundström, V.; Yamane, T.; Rentzepis, P. M. *Biophys. J.* **1978**, *22*, 121.
- (76) Waddell, W.; Schaeffer, A. M.; Becker, R. S. *J. Am. Chem. Soc.* **1973**, *95*, 8223.
- (77) Yoshihara, K.; Namiki, A.; Sumitani, M.; Nakashima, N. *J. Chem. Phys.* **1979**, *71*, 2892.
- (78) Sundström, V.; Gillbro, T. *J. Phys. Chem.* **1982**, *86*, 1788.